The Journal of Neuroscience, December 15, 2001, 21(24):9629–9637

Glycosylation Alters Steady-State Inactivation of Sodium Channel $Na_v1.9$/NaN in Dorsal Root Ganglion Neurons and Is Developmentally Regulated

Lynda Tyrrell,[1,2,3] Muthukrishnan Renganathan,[1,2,3] Sulayman D. Dib-Hajj,[1,2,3] and Stephen G. Waxman[1,2,3]

[1]Department of Neurology and [2]Paralyzed Veterans of America/Eastern Paralyzed Veterans Association Neuroscience Research Center, Yale University School of Medicine, New Haven, Connecticut 06510, and [3]Rehabilitation Research Center, Veterans Administration Connecticut Healthcare System, West Haven, Connecticut 06516

Na channel NaN ($Na_v1.9$) produces a persistent TTX-resistant (TTX-R) current in small-diameter neurons of dorsal root ganglia (DRG) and trigeminal ganglia. $Na_v1.9$-specific antibodies react in immunoblot assays with a 210 kDa protein from the membrane fractions of adult DRG and trigeminal ganglia. The size of the immunoreactive protein is in close agreement with the predicted $Na_v1.9$ theoretical molecular weight of 201 kDa, suggesting limited glycosylation of this channel in adult tissues. Neonatal rat DRG membrane fractions, however, contain an additional higher molecular weight immunoreactive protein. Reverse transcription-PCR analysis did not show additional longer transcripts that could encode the larger protein. Enzymatic deglycosylation of the membrane preparations converted both immunoreactive proteins into a single faster migrating band, consistent with two states of glycosylation of $Na_v1.9$. The developmental change in the glycosylation state of $Na_v1.9$ is paralleled by a developmental change in the gating of the persistent TTX-R Na^+ current attributable to $Na_v1.9$ in native DRG neurons. Whole-cell patch-clamp analysis demonstrates that the midpoint of steady-state inactivation is shifted 7 mV in a hyperpolarized direction in neonatal (postnatal days 0–3) compared with adult DRG neurons, although there is no significant difference in activation. Pretreatment of neonatal DRG neurons with neuraminidase causes an 8 mV depolarizing shift in the midpoint of steady-state inactivation of $Na_v1.9$, making it indistinguishable from that of adult DRG neurons. Our data show that extensive glycosylation of rat $Na_v1.9$ is developmentally regulated and changes a critical property of this channel in native neurons.

Key words: spinal sensory neurons; ion channel; tetrodotoxin resistant; persistent Na current; desialidation; voltage clamp

Voltage-gated Na channels are multimers that consist of the pore-forming α-subunit and auxiliary β-subunits (Catterall, 2000). Ten distinct α-subunits have been identified in rat, with homologs from mammalian species, including humans (Goldin et al., 2000; Goldin, 2001). Na channel α-subunits are expressed in a tissue-specific and developmentally specific manner (Beckh et al., 1989; Akopian et al., 1996; Felts et al., 1997; Dib-Hajj et al., 1998; Schaller and Caldwell, 2000).

Many Na channels are heavily glycosylated (Barchi et al., 1980; Miller et al., 1983; Messner and Catterall, 1985; Schmidt and Catterall, 1986, 1987). The carbohydrate moiety accounts for 15–30% of the mass of rat brain and skeletal muscle and eel α-subunits (Miller et al., 1983; Messner and Catterall, 1985) but only 5% of rat cardiac α-subunit (Cohen and Barchi, 1993). Cotranslational glycosylation is important for α-subunit folding and interaction with auxiliary subunits (Schmidt and Catterall, 1987). Subsequent post-translational addition of sialic acid accounts for the bulk of the carbohydrate glycocalyx of brain, skeletal muscle, and eel channels (Miller et al., 1983; Messner and Catterall, 1985). Inhibition of sialic acid addition does not affect the assembly of functional channels in the cell membrane (Schmidt and Catterall, 1987); however, such inhibition or enzymatic desialidation modifies the gating properties of Na channels (Recio-Pinto et al., 1990; Bennett et al., 1997; Zhang et al., 1999).

Glycosylation has been shown to modulate the gating properties of eel Na channels reconstituted in lipid bilayers (Recio-Pinto et al., 1990) and recombinant skeletal ($Na_v1.4$) and cardiac ($Na_v1.5$) channels expressed in mammalian cell lines (Bennett et al., 1997; Zhang et al., 1999). Bennett et al. (1997) documented a depolarizing shift of activation and inactivation after desialidation, whereas Zhang et al. (1999) documented a depolarizing shift of activation but a smaller hyperpolarizing shift of inactivation. None of these studies, however, investigated the effect of deglycosylation within native cells. The physiological properties of Na channels can vary, depending on the cell type in which they are expressed, and can differ significantly for a channel expressed in mammalian cell lines versus neurons (Cummins et al., 2001). Voltage-gated K^+ channels $K_v1.1$ and $K_v1.2$ from brain possess a different glycocalyx from recombinant channels expressed in the COS-1 cell line (Shi and Trimmer, 1999). Thus, the effects of glycosylation of voltage-gated channels in native tissues may differ from those in cell lines.

$N_v1.9$/NaN is expressed preferentially in small dorsal root ganglion (DRG) and trigeminal ganglion neurons and their axons (Dib-Hajj et al., 1998; Fjell et al., 2000). $Na_v1.9$ channels are

Received Aug. 9, 2001; revised Sept. 21, 2001; accepted Sept. 27, 2001.

This work was supported in part by grants from the National Multiple Sclerosis Society and the Rehabilitation Research and Development Service and Medical Research Services, Department of Veterans Affairs, and by gifts from the Paralyzed Veterans of America and Eastern Paralyzed Veterans Association. We also thank the Blinded Veterans of America for their support. We thank Dr. Joel A. Black and William N. Hormuzdiar for providing tissues and cultures, Dr. Ted Cummins for helpful discussions, and Bart Toftness for technical assistance.

Correspondence should be addressed to Dr. Sulayman D. Dib-Hajj, Paralyzed Veterans of America/Eastern Paralyzed Veterans Association Neuroscience Research Center (127A), Veterans Administration Medical Center, Building 34, 950 Campbell Avenue, West Haven, CT 06516. E-mail: sulayman.dib-hajj@yale.edu.

 0270-6474/01/219629-09$15.00/0

resistant to tetrodotoxin (TTX-R) and produce Na currents that are persistent at −70 to −60 mV, with wide overlap between activation and steady-state inactivation (Cummins et al., 1999). As predicted from these properties, $Na_v1.9$ appears to contribute to setting the resting membrane potential and to subthreshold electrogenesis (Herzog et al., 2001).

This study shows that $Na_v1.9$ is present in two glycosylated states at early neonatal ages but in only a lightly glycosylated state in adults. Heavier glycosylation may contribute to a hyperpolarized shift in steady-state inactivation of $Na_v1.9$ in neonatal compared with adult neurons. Pretreatment of cultured neurons by neuraminidase, which removes sialic acid residues, abolishes this shift. These findings document the first case of developmental regulation of glycosylation of a Na channel and demonstrate a functional correlate of differential glycosylation of channels in their native environment.

MATERIALS AND METHODS

Animals. Adult, timed-pregnant and postnatal [postnatal day 0 (P0), P2, P3, P4, P7, and P21] Sprague Dawley rats were used to harvest tissue. Adult Sprague Dawley female rats were used to investigate the effect of axotomy on $Na_v1.9$ protein levels. Axotomy was performed as described previously (Dib-Hajj et al., 1996, 1998). Briefly, Sprague Dawley female rats were anesthetized with ketamine (40 mg/kg, i.p.) and xylazine (2.5 mg/kg, i.p). Sciatic nerves at midthigh level were exposed on the right side, ligated with 4–0 sutures proximal to the pyriform ligament, transected, and placed in a silicon cuff to prevent regeneration (Fitzgerald et al., 1985). Fourteen days after axotomy, the rats were anesthetized, and control (contralateral) and injured (ipsilateral) L4/L5 DRG were removed for analysis. Experiments were performed in accordance with NIH guidelines for the care and use of laboratory animals.

Preparation of membrane fraction. The fourth and fifth lumber DRG (L4 and L5), trigeminal ganglia, spinal cord, and liver tissues were dissected from Sprague Dawley rats and either processed immediately or snap frozen in liquid nitrogen and kept at −80°C for future processing. Tissues were homogenized in a glass dounce in ice-cold lysis buffer at 30 μl/mg tissue. The lysis buffer (0.3 M sucrose, 10 mM Tris, pH 8.1, and 2 mM EDTA) was supplemented with protease inhibitors: 1 mM PMSF, 10 μg/ml aprotinin, 10 μg/ml leupeptin, 1 mM DTT, 1 mM benzamidine, 1 mM pepstatin, 8 μg/ml calpain 1, and 8 μg/ml calpain 11). Homogenates were kept on ice for 1 hr before centrifugation at 1000 × *g* (low-speed spin) for 7 min at 4°C to remove nuclei and intact cells. The pellet was rehomogenized and spun again under the same conditions. The supernatants from the two low-speed spins were combined and centrifuged at 120,000 × *g* for 1 hr at 4°C. The pellet, containing the total membrane fraction, was suspended in 0.2 M KCl and 10 mM HEPES, pH 7.4.

To solubilize the membrane fraction, an equal volume of 5% Triton X-100 and 10 mM HEPES, pH 7.4, was added to the sample, and the suspension was kept on ice for 1 hr. The unsolubilized material was pelleted by centrifugation at 10,000 × *g* for 10 min at 4°C, and the soluble material in the supernatant was collected for additional processing. Protein content was determined using Bio-Rad (Hercules, CA) DC assay for high detergent samples.

Antibodies. An anti-$Na_v1.9$ polyclonal antibody was raised in rabbits against the C-terminal 18 amino acid peptide (CNGDLSSLDVAKVKVHND) and affinity purified over the specific peptide column (Fjell et al., 2000). Anti-$Na_v1.9$ antibody was used at a final concentration of 0.2 μg/ml. A generic Na channel antibody against an 18 amino acid, highly conserved peptide (TEEQKKYYNAMKKLGSKK) in the cytoplasmic loop connecting domains 3 and 4 (L3) of the channel was obtained from Upstate Biotechnology (Lake Placid, NY) and used at a final concentration of 2 μg/ml.

Immunoblot assay. Samples (10–20 μg) were denatured in Laemmli's sample buffer for 20 min at 37°C. Proteins were fractionated by SDS-PAGE using either 5 or 4–15% gradient Tris-HCl Ready gels (Bio-Rad) and then electrotransferred to Immobilon-P membrane (Millipore, Bedford, MA) overnight at 22 mV and 4°C. Blots were blocked with 10% dried milk in TBS for 1 hr at room temperature before incubation for 2 hr at room temperature with the primary antibody diluted in 5% BSA in TBS. Blots were washed extensively in TBST (TBS plus 0.2% Tween 20). Immunoreactive proteins were detected by incubating with a 1:10,000 dilution in 1.25% BSA of a goat anti-rabbit IgG secondary antibody conjugated to horseradish peroxidase (Dako, Glostrup, Denmark) for 1 hr at room temperature. The signal was detected by Renaissance chemiluminescence according to the recommendations of the manufacturer (NEN, Boston, MA).

Deglycosylation of membrane fractions. The membrane fraction of L4 and L5 DRG from three to five rats at different postnatal ages were prepared as described above. The membrane pellet was suspended in 10 μl of 0.2 M KCl and 10 mM HEPES, pH 7.4, SDS was added to a final concentration of 0.3%, and the sample was heated to 37°for 15 min. After cooling on ice, 4 vol of a buffer containing 40 mM sodium phosphate, pH 7.0, 10 mM EDTA, 0.6% Triton X-100, and 1% β-mercaptoethanol were added, followed by 1 μl (500 U) of the N-glycosidase PNGase F (New England Biolabs, Beverly, MA) and incubated at 37°C for 1 hr. This enzyme cleaves the glycosidic bond between the N-acetylglucosamine (GlcNAc) group and the asparagine residue of N-linked glycoproteins. A control sample was prepared without the addition of PNGase. Ten microliters of a 6× sample buffer was added to the reaction, and the sample was denatured and the proteins were fractionated on a gradient gel as described above.

DRG primary cultures. Neonatal and adult animals were decapitated, and L4 and L5 DRG were quickly removed and desheathed in sterile complete saline solution (CSS), pH 7.2. The DRG were then enzymatically digested at 37°C for 20 min with collagenase A (1 mg/ml; Roche, Indianapolis, IN) in CSS and for 15 min with collagenase D (1 mg/ml; Roche) and papain (30 U/ml; Worthington, Lakewood, NJ) in CSS at 37°C. The DRG were gently centrifuged (100 × *g* for 3 min), and the pellets were triturated in DRG media (1:1 DMEM/ F12, 10% FCS, 100 U/ml penicillin, and 0.1 mg/ml streptomycin) containing 1 mg/ml BSA (Fraction V; Sigma, St. Louis, MO) and 1 mg/ml trypsin inhibitor (Sigma). The cells were then plated on poly-ornithine–laminin-coated glass coverslips, flooded with DRG media after 1 hr, and incubated at 37°C in a humidified 95% air–5% CO_2 incubator.

Desialidation of Na channels. Neonatal (P0–P3) and adult DRG cultures were enzymatically treated to remove sialic acid residues from the carbohydrate moiety of membrane proteins. Neuraminidase treatment was performed as described previously (Zhang et al., 1999). Briefly, DRG cultures were treated with 0.3 U/ml (800 U/mg protein) neuraminidase type X (Sigma) for 3–5 hr at 37°C before the electrophysiological recordings were made. Drugs were washed out immediately before recording with the bath solution listed below. Sister cultures that were not treated by neuraminidase served as controls.

Electrophysiological recordings. This study focused on the small-diameter C-type DRG neurons that produce the persistent TTX-R Na^+ currents attributable to $Na_v1.9$ (Cummins et al., 1999; Dib-Hajj et al., 1999a). Na current properties in DRG neurons were investigated 2–8 hr after plating. DRG neurons displayed only short (<10 μm) axonal processes during the short period of culture, facilitating the voltage clamp.

Coverslips carrying cultured DRG neurons were mounted in a small flow-through chamber on the microscope stage and were continuously perfused with bath external solution (see below) with a push–pull syringe pump (World Precision Instruments, Saratoga, FL). Cells were voltage clamped via the whole-cell configuration with an Axopatch-200B amplifier (Axon Instruments, Foster City, CA) using standard techniques. For currents >20 nA, we switched to the 50 MΩ feedback resistor (β of 0.1), which can pass up to 200 nA. Micropipettes (0.4–0.6 MΩ) were pulled from borosilicate glasses (Boralex) with a Flaming Brown P80 micropipette puller, polished on a microforge, and coated with a mixture prepared of three parts of finely shredded parafilm and one part each of light and heavy mineral oil (Sigma) to reduce the pipette capacitance. The average series resistance was 0.74 ± 0.04 MΩ (n = 72). Capacity transients were cancelled, and series resistance was compensated (90%) as necessary. The pipette solution contained (in mM): 140 CsF, 1 EGTA, 10 NaCl, and 10 HEPES, pH 7.3 (adjusted to 310 mOsm/l with glucose). The bath solution contained (in mM): 140 NaCl, 3 KCl, 1 $MgCl_2$, 1 $CaCl_2$, 0.1 $CdCl_2$, and 20 HEPES, pH 7.3 (adjusted to 320 mOsm/l with glucose). $CdCl_2$ was used to block Ca^{2+} currents. The pipette potential was zeroed before seal formation, and voltages were not corrected for liquid junction potential. Leakage current was digitally subtracted on-line using hyperpolarizing control pulses, applied before the test pulse, of one-sixth test pulse amplitude (−P/6 procedure). Whole-cell currents were filtered at 5 kHz and acquired at 50 kHz using Clampex 8.1 software (Axon Instruments). For current density measurements, membrane currents were normalized to membrane capacitance,

which was calculated as the integral of the transient current in response to a brief hyperpolarizing pulse from −120 (holding potential) to −130 mV. All experiments were performed at room temperature (21–25°C).

Separation of slow and persistent TTX-R Na^+ currents using prepulse inactivation. Prepulse inactivation takes advantage of the differences in the inactivation properties of the slow and persistent TTX-R Na^+ currents (Cummins et al., 1999). TTX at 300 nM was included in the bath solution to isolate slow and persistent TTX-R currents from fast TTX-sensitive (TTX-S) Na^+ currents (which are completely blocked by this TTX concentration). Na^+ currents were evoked from a holding potential of −130 mV to test pulses ranging from −100 to +60 mV in 5 mV steps. Persistent TTX-R Na^+ current was obtained by subtracting the current obtained after a −50 mV prepulse (500 msec duration), which elicits only slow Na^+ current, from the current obtained with the more hyperpolarized prepulse (−130 mV), which elicits both slow and persistent TTX-R Na^+ currents.

Conductance was determined as $I_p/(V_R - V)$, where I_p is the peak inward current, V_R is the reversal potential, and V is the test pulse voltage. V_R was determined by fitting the normalized Na^+ current voltage (I/I_{max}) relationships to the following Boltzmann equation:

$$I/I_{max} = \frac{1}{1 + (\exp((V_{1/2} - V)/k)) \times G_i \times (V - V_R)}$$

where $V_{1/2}$ is the voltage for half-maximal activation in millivolts, V is the test pulse voltage, k is the corresponding slope factor, and G_i is a scaling factor with the dimensions of a conductance.

Normalized conductance (G/G_{max}) was fit with a single Boltzmann relationship of the following form:

$$G/G_{max} = \frac{1}{1 + \exp[(V - V_{1/2})/k]}$$

where V is the test pulse voltage, $V_{1/2}$ is the voltage for half-maximal activation in millivolts, and k is the corresponding slope factor.

Steady-state voltage-dependent inactivation curves were measured using 500 msec prepulses to the indicated potentials, followed by a test pulse to −50 mV, in which no activation of slow Na^+ current occurs. Peak test pulse current was plotted as a function of prepulse potential, normalized, and fit with a single Boltzmann function:

$$I = \frac{1}{1 + \exp[(V_{pp} - V_h)/k_h]},$$

where V_{pp} is the prepulse potential, V_h is the midpoint potential, and k_h is the corresponding slope factor.

Data analysis. Patch-clamp data were analyzed using a combination of Clampfit 8.1 software (Axon Instruments) and Origin (Microcal Software Inc., Northampton, MA). Student's unpaired t test was used for statistical analysis of the data. All p values were significant at the 0.05 level or better. Data are presented as mean ± SEM.

RESULTS

Characterization of $rNa_v1.9$-specific antibody

A polyclonal antibody was raised against the C-terminal peptide sequence of $Na_v1.9$, and the affinity-purified antisera was used successfully to localize this channel to rat small-diameter $IB4^+$ DRG sensory neurons (Fjell et al., 2000). We further characterized this antibody in immunoblot assays (Fig. 1). An immunoreactive protein of an apparent molecular weight of ~210 kDa, which is in close agreement with the predicted molecular weight of $Na_v1.9$ (Dib-Hajj et al., 1998), is detected in membrane fractions of adult rat DRG and trigeminal ganglia but not from liver or spinal cord (Fig. 1*A*). A smaller protein of ~100 kDa is detected in most of the samples but is also detectable when the primary antibody was omitted from the assay (data not shown), indicating that it is a nonspecific product. To confirm the presence of proteins in the spinal cord sample, the blot was stripped and reprobed with a generic Na channel antibody (Fig. 1*B*). Multiple immunoreactive bands are detected in the DRG and trigeminal ganglia (Fig. 1*B*), consistent with the expression of multiple Na channels in these tissues (Akopian et al., 1996; Black et al., 1996; Dib-Hajj et al., 1998; Kim and Chung, 1999). A major immunoreactive band, which migrates much slower than the 209 kDa marker, is observed in the spinal cord (Fig. 1*B*), consistent with the presence of brain-type channels (Felts et al., 1997), which are heavily glycosylated (Messner and Catterall, 1985). Immunoblots of membrane fractions of 24 hr DRG cultures show the presence of a single ~210 kDa immunoreactive band (Fig. 1*C*). The presence of the 210 kDa immunoreactive protein in cultured DRG neurons, at a time in culture when a substantial persistent TTX-R Na^+ current attributable to $Na_v1.9$ is detected (Cummins et al., 1999) and immunostaining of small DRG neurons with this antibody has been shown (Fjell et al., 2000; Sleeper et al., 2000), are consistent with the conclusion that it represents $Na_v1.9$ in both the cultured DRG and native tissue. Interestingly, the nonspecific band at ~100 kDa is not detected in the DRG culture sample, further supporting the conclusion that it is unrelated to $Na_v1.9$.

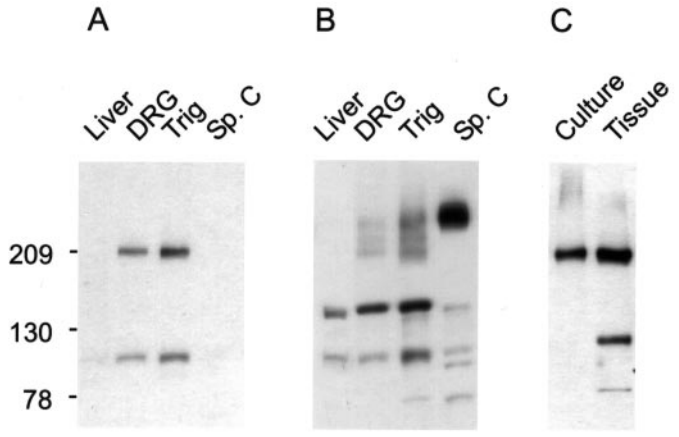

Figure 1. Immunoblot assay to show specificity of anti-$Na_v1.9$ antibody. *A*, An immunoreactive band of molecular weight ~210 kDa is detected in DRG and trigeminal (*Trig.*) ganglia but not in spinal cord (*Sp. C*) or liver. A much smaller nonspecific protein of molecular weight ~100 kDa is detected in some samples. *B*, The blot was stripped and reprobed with a generic sodium channel antibody. DRG, trigeminal, and spinal cord samples show multiple immunoreactive bands, consistent with the presence of multiple sodium channels in these tissues. A number of smaller proteins are also detected and are the result of nonspecific interaction with the secondary antibody. *C*, Membrane fractions from adult DRG (*Tissue*) and from 24 hr cultured DRG cells (*Culture*). A single immunoreactive band of ~210 kDa is detected in the cultured DRG sample, consistent with the conclusion that the ~100 kDa protein is unrelated to $Na_v1.9$. Positions of molecular weight markers 209, 130, and 78 kDa are indicated.

Transcripts of $Na_v1.9$ as well as the persistent TTX-R Na current that is attributable to this channel are downregulated in DRG neurons after transection of their peripheral projections in the sciatic nerve (Dib-Hajj et al., 1998; Sleeper et al., 2000). Recently, we showed that there is a reduction in the $Na_v1.9$ immunostaining of axotomized DRG neurons using this $Na_v1.9$-specific antibody (Sleeper et al., 2000). We now report a similar finding in an immunoblot assay of DRG tissue 14 d after axotomy, using this $Na_v1.9$-specific antibody. Figure 2 shows an immunoblot assay using the membrane fractions of rat DRG tissues contralateral and ipsilateral to axotomy. The 100 kDa band serves as a convenient internal control to demonstrate equal loading of protein per lane. The intensities of the $Na_v1.9$ bands (Fig. 2) were determined by densitometry and show that injury resulted in a 31

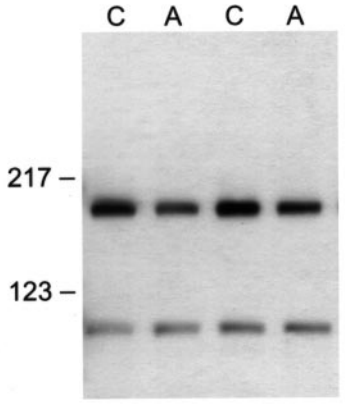

Figure 2. Axotomy reduces the level of $Na_v1.9$ protein in rat DRG. The sciatic nerves of the right side of four rats were transected, and the level of $Na_v1.9$ protein in the axotomized DRG (*A*) was compared with that in the intact ganglia (*C*) 14 d after axotomy in an immunoblot assay. The L4 and L5 DRG from the intact (*C*) and from the axotomized (*A*) sides were pooled from two rats, and the membrane fraction was analyzed using the $Na_v1.9$-specific antibody. The intensity of the bands was determined by densitometry. Axotomy results in a clear reduction of the level of $Na_v1.9$ protein in axotomized DRG. The nonspecific ~100 kDa protein serves as a convenient marker to demonstrate equal loading of the gel. Positions of molecular weight markers 217 and 123 kDa are indicated.

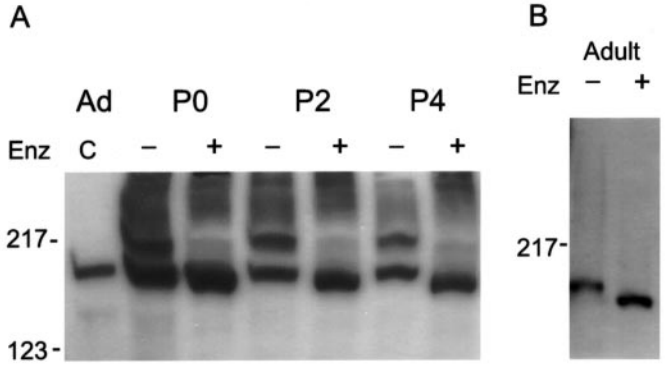

Figure 4. Both $Na_v1.9$ immunoreactive proteins are glycosylated. *A*, Treatment of the membrane fractions from P0, P2, and P4 DRG with the glycosidase PNGase F (*Enz*) converts the immunoreactive proteins into a single faster migrating species. Samples were separated on a 4–15% gradient gel before electroblotting. *Ad* shows the immunoreactive protein from untreated adult DRG sample. *B*, Similar treatment of the membrane fraction from adult DRG converts the ~210 kDa protein into a faster migrating species. Samples were separated on a 5% gel before electroblotting. The + and − *signs* indicate treated and untreated samples, respectively.

and 38% reduction of the $Na_v1.9$ signal in two experiments in which axotomized and control DRG were processed in parallel (see Materials and Methods).

Immunoblot analysis of $Na_v1.9$ reveals developmental regulation of the glycosylation of this channel

Immunoblot analysis of the membrane fraction shows that P3 DRG and trigeminal ganglia contain two immunoreactive bands compared with a single band in adult tissue (Fig. 3*A*). The immunoreactive band in adult tissue comigrates with the smaller of the two bands in the P3 tissue. Because the peptide used in the production of this antibody consists of the C-terminal 18 amino acid residues of $Na_v1.9$, a protein with additional sequence encoding a longer N-terminal polypeptide, interdomain cytoplasmic loops, or an insertion into the C-terminal polypeptide could account for the higher molecular weight immunoreactive protein. To examine these possibilities, we performed reverse transcription-PCR analysis on adult and P3 DRG and trigeminal ganglia templates, which did not show a difference in the length of the amplicons that encode these regions of the channel (data not shown). Therefore, a developmentally regulated post-translational modification of $Na_v1.9$ is the most likely source of the higher molecular weight immunoreactive protein in the P3 tissue.

Membrane fractions from DRG and trigeminal ganglia at different developmental stages were analyzed by a similar immunoblot assay using the $Na_v1.9$-specific antibody. Immunoblot analysis of membrane fraction from DRG shows a 210 kDa immunoreactive protein at embryonic day 17 (E17), in addition to a higher molecular weight protein that becomes prominent at P0 but declines by P7 and is not detectable by P21 (Fig. 3*B*). A similar pattern is seen in trigeminal ganglia at these developmental stages (Fig. 3*B*).

Na channels from adult brain and skeletal and cardiac muscles are known to be glycosylated. The apparent molecular weight (~210 kDa) of $Na_v1.9$ is ~5% higher than the theoretical molecular weight of 201 kDa (Dib-Hajj et al., 1998). The additional mass could be attributable to glycosylation of this channel. We reasoned that the increased mass of the additional immunoreactive protein in the neonatal tissue is attributable to a heavily glycosylated form of $Na_v1.9$. To test this hypothesis, membrane fractions of DRG were treated with the glycosidase enzyme PNGase F and analyzed by immunoblot assay. PNGase F cleaves the glycosidic bond of N-acetylglucosamine that is linked to the aspargine (N) side chain of N-glycosylated proteins. Figure 4*A* shows the effect of the enzymatic treatment of the membrane fractions from P0, P2, and P4 on the size of $Na_v1.9$ protein in these tissues. The enzymatic treatment converted both immuno-

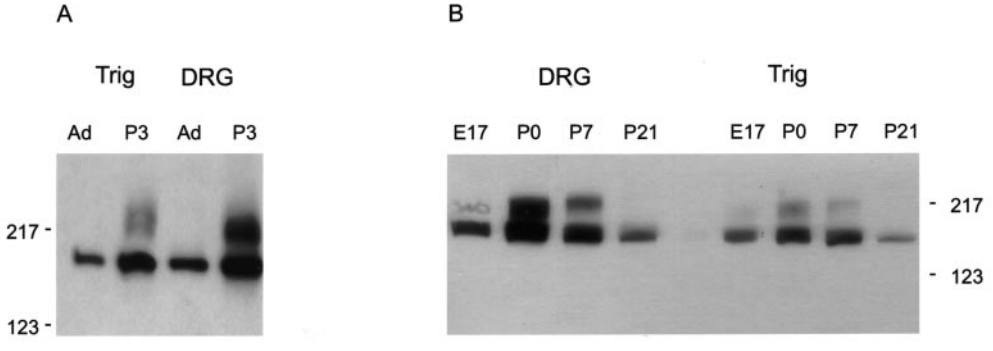

Figure 3. Two $Na_v1.9$ immunoreactive bands are present in neonatal rat DRG. *A*, Membrane fractions from DRG and trigeminal ganglia (*Trig*) of P3 and adult (*Ad*) rats were probed with the $Na_v1.9$ antibody and show an additional, higher molecular weight immunoreactive protein in the P3 sample compared with the adult sample. *B*, DRG and trigeminal ganglia membrane fractions from P0 and P7 rats contain two immunoreactive proteins. Trace amount of the slower migrating band is present in the E17 sample, whereas the P21 DRG sample contains only the faster migrating species.

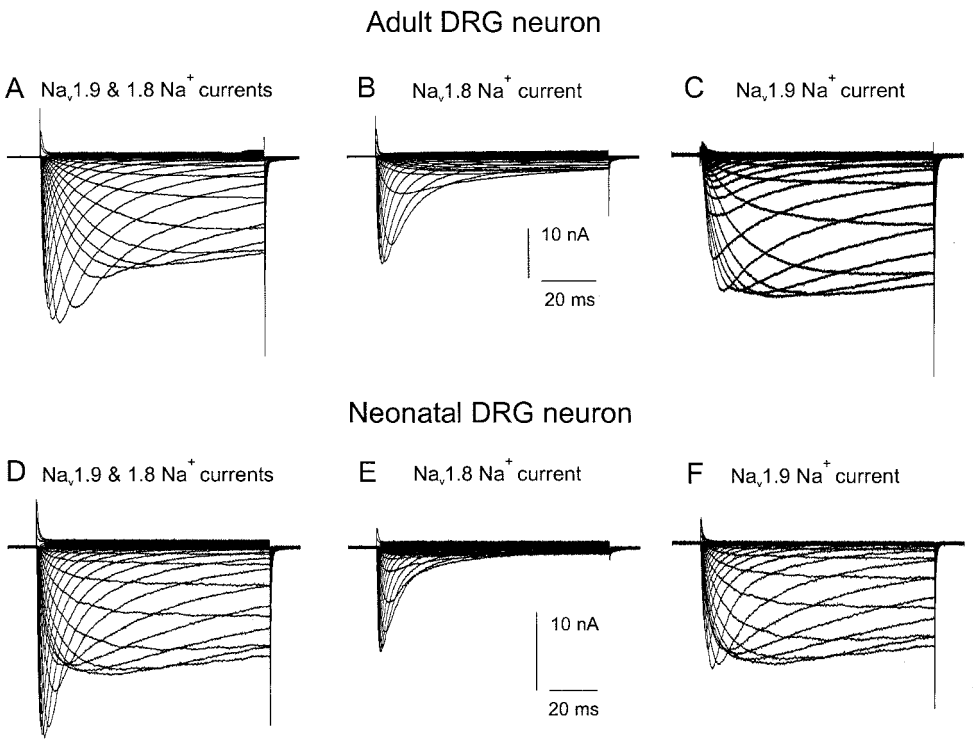

Figure 5. Separation of $Na_v1.9$ Na^+ currents from $Na_v1.8$ Na^+ currents by prepulse subtraction in adult and neonatal DRG neurons. *A*, Families of Na^+ current traces from an adult small-diameter DRG neuron in the presence of 300 nM TTX. The capacitance of the adult DRG neuron was 13.31 pF. Both $Na_v1.9$ Na^+ current and $Na_v1.8$ Na^+ current were elicited in response to 100 msec test pulses from a holding potential of −130 mV to test potentials ranging from −100 to + 60 mV in 5 mV steps. *B*, The same neuron when given a prepulse of −50 mV for 500 msec before the test potentials from −100 to +60 mV elicited only $Na_v1.8$ Na^+ currents. *C*, Subtraction of current traces shown in *B* from the current traces shown in *A* yields $Na_v1.9$ Na^+ currents. *D–F* represent separation of $Na_v1.9$ Na^+ currents from $Na_v1.8$ Na^+ currents in a neonatal DRG neuron as shown in *A–C*. The capacitance of the neonatal DRG neuron was 7.13 pF.

reactive proteins to a faster migrating band compared with the untreated sample. This clearly shows that even the 210 kDa protein is itself glycosylated. Figure 4*B* shows the mobility shift of the immunoreactive protein after the treatment of adult DRG fractions with PNGase F, also indicating that the adult isoform is lightly glycosylated.

Isolation of $Na_v1.9$ Na^+ currents in adult and neonatal DRG neurons

Slow and persistent TTX-R Na^+ currents produced by $Na_v1.8$/SNS and $Na_v1.9$/NaN channels, respectively (Cummins et al., 1999; Dib-Hajj et al., 1999a), are observed in adult (Fig. 5*A*) and neonatal (Fig. 5*D*) DRG neurons. These two types of currents can be separated by a prepulse protocol (Cummins et al., 1999). The mean peak persistent TTX-R Na^+ current density normalized to capacitance for adult and neonatal DRG neurons are 0.79 ± 0.1 (n = 30) and 0.67 ± 0.07 (n = 29) nA/pF, respectively. The decrease in neonatal persistent TTX-R Na^+ current density is not statistically significant ($p > 0.05$). The capacitance of adult and neonatal DRG neurons are 19.55 ± 1.83 and 17.22 ± 1.32 pF, respectively, which are also not significantly different ($p > 0.05$). The adult persistent TTX-R Na^+ current density is consistent with the results obtained in other studies (Cummins et al., 1999, 2000; Renganathan et al., 2000a,b).

Activation and steady-state inactivation of persistent TTX-R Na^+ current in adult and neonatal neurons

The current–voltage relationships for the persistent TTX-R Na^+ currents in adult (*open circles*) (n = 30) and neonatal (*filled circles*) (n = 29) DRG neurons (Fig. 6*A*) are similar and suggest that the additional glycosylation in neonatal $Na_v1.9$ channels does not have an effect on this relationship. The persistent TTX-R Na^+ current in adult and neonatal neurons activates between −80 and −70 mV, peaks at approximately −40 mV, and reverses at +50 mV. The midpoint voltages ($V_{1/2}$) and slope for activation of adult and neonatal persistent TTX-R Na^+ currents were obtained from fitting the conductance–voltage curve with the Boltzmann equation (Fig. 6*B*). The $V_{1/2}$ and slope for activation of adult persistent TTX-R Na^+ current are −57.3 ± 1.1 mV and 6.2 ± 0.5 mV/*e*-fold (*open circles*) (n = 30) and, for neonatal persistent TTX-R Na^+ current, are −54.2 ± 0.9 mV and 6.6 ± 0.4 mV/*e*-fold (*filled circles*) (n = 29), respectively. The 3 mV difference in the $V_{1/2}$ did not reach statistical significance ($p > 0.05$). These results suggest that the presence of negative charges attributable to sialidation does not influence activation properties of the persistent TTX-R Na^+ current.

We next compared the steady-state inactivation of adult and neonatal persistent TTX-R Na^+ current (Fig. 6*C*). The $V_{1/2}$ and slope for steady-state inactivation of the adult TTX-R persistent Na^+ current are −48.2 ± 1.3 mV and 6.0 ± 0.3 mV/*e*-fold (*open circles*) (n = 30), respectively, whereas those of the neonatal persistent TTX-R Na^+ current are −55.2 ± 1.3 mV and 6.5 ± 0.4 mV/*e*-fold, respectively (*filled circles*) (n = 29). The $V_{1/2}$ but not the slopes of neonatal and adult persistent TTX-R Na^+ currents are significantly different ($p < 0.001$). Thus, $V_{1/2}$ of the steady-state inactivation of the persistent TTX-R Na^+ current of neonatal neurons is shifted by ~7 mV in the hyperpolarizing direction relative to that of adult DRG neurons. These results suggest that the presence of negative charges attributable to the terminal sialic acid residues on the glycocalyx influences the steady-state inactivation of the neonatal persistent TTX-R Na^+ current.

Enzymatic desialidation of neonatal persistent TTX-R Na^+ channels does not affect activation

Sialic acid is a prominent constituent of glycosylation of neuronal and muscle Na channels (Miller et al., 1983; Messner and Catterall, 1985; Roberts and Barchi, 1987). Therefore, we hypothesized that the additional glycosylation of neonatal $Na_v1.9$ channel protein might carry extra negative charges. We investigated the

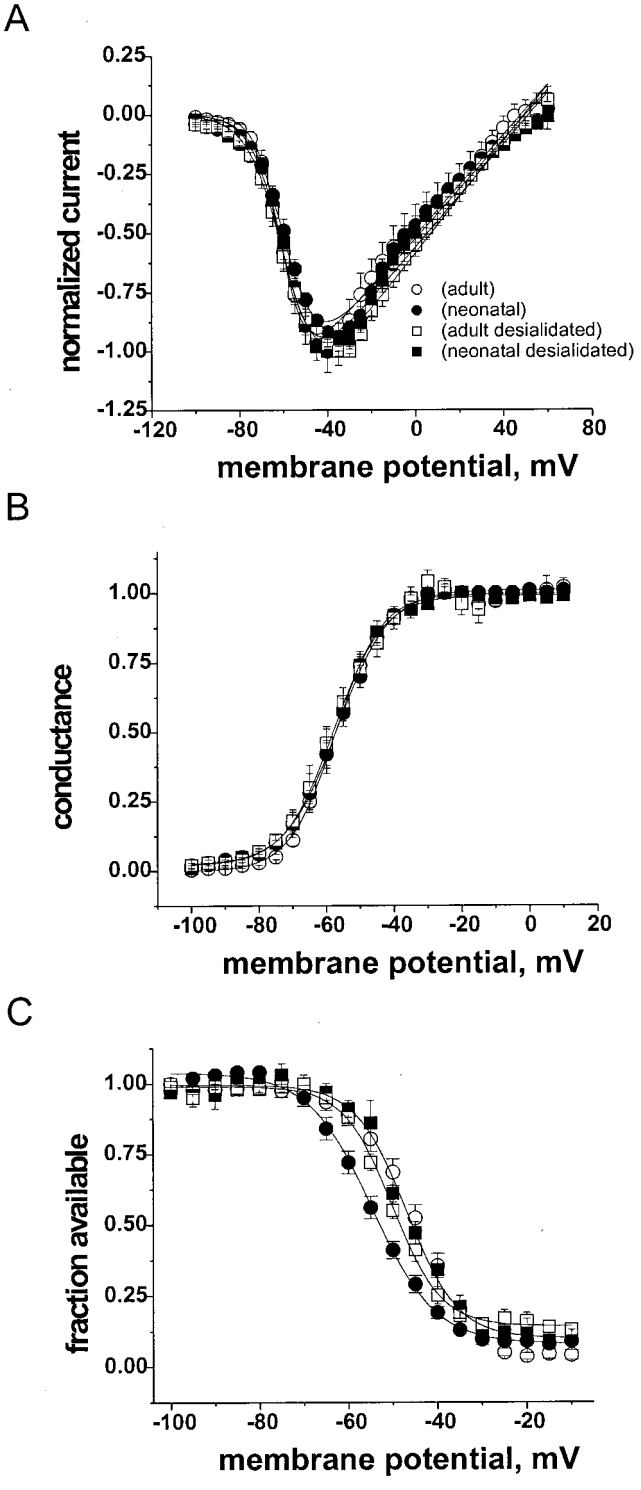

Figure 6. Desialidation affects the steady-state inactivation of $Na_v1.9$ Na^+ currents only in neonatal DRG neurons. *A*, Normalized current–voltage curves for neonatal (*filled circles*), adult (*open circles*), neonatal desialidated (*filled squares*), and adult desialidated (*open squares*) $Na_v1.9$ Na^+ currents are shown in *A*. Current values were normalized to the peak value obtained at −40 mV. *Symbols* are the same for *B* and *C* and are shown also in the figure for clarity. *B*, Desialidation did not affect voltage dependence of activation of neonatal $Na_v1.9$ Na^+ currents. Voltage dependence of activation of neonatal, adult, neonatal desialidated, and adult desialidated $Na_v1.9$ channels are shown. *C*, Desialidation causes a depolarizing shift of steady-state inactivation of neonatal $Na_v1.9$ Na^+ currents. Steady-state voltage dependence of inactivation of neonatal, adult, neonatal desialidated, and adult desialidated $Na_v1.9$ channels are shown. *Lines* are the Boltzmann fits to the data. The values of $V_{1/2}$ and slope from Boltzmann fits of steady-state activation and steady-state inactivation of pooled neonatal, adult, neonatal desialidated, and adult desialidated $Na_v1.9$ Na^+ currents are shown in Table 1.

effect of different degrees of glycosylation on the voltage dependence of $Na_v1.9$ channel gating by comparing the voltage dependence of activation and steady-state inactivation in neonatal and adult neurons. To test whether sialic acid residues affect the voltage dependence of $Na_v1.9$ gating, we pretreated DRG neurons in culture with neuraminidase to remove the sialic acid from Na channels. Removal of negatively charged sugar residues on the extracellular face of Na channels by desialidation reduces the surface potential and has been shown to affect $Na_v1.4$ and $Na_v1.5$ gating (Bennett et al., 1997; Zhang et al., 1999).

The current–voltage relationship for the persistent TTX-R Na^+ current for neuraminidase-treated neonatal DRG neurons is shown in Figure 6*A* (*filled squares*) ($n = 15$), and it is similar ($p > 0.05$) to that for control nontreated neonatal DRG neurons (*filled circles*) ($n = 36$). The persistent TTX-R Na^+ current density and capacitance of neonatal DRG neurons after the neuraminidase treatment are 0.63 ± 0.08 nA/pF and 15.34 ± 1.3 pF, respectively. The current density and cell capacitance are similar between treated and nontreated neonatal control neurons, suggesting that desialidation does not affect the production of functional, membrane-bound $Na_v1.9$ channel complexes.

The activation curves for neuraminidase-treated neonatal DRG neurons are shown in Figure 6*B* (*filled squares*) ($n = 15$). The mean $V_{1/2}$ values and slopes obtained from Boltzmann fits of steady-state activation data are −57.5 ± 2.2 mV and 5.84 ± 0.8 mV/*e*-fold, respectively, and are similar to the values −54.2 ± 1.2 mV and 6.62 ± 0.4 mV/*e*-fold obtained for nontreated neonatal DRG neurons (Table 1). These results further validate the conclusion (see above) that the increased glycosylation of neonatal $Na_v1.9$ does not affect the steady-state activation properties of the persistent TTX-R Na^+ current in native neurons.

Enzymatic desialidation of neonatal persistent TTX-R Na^+ channels causes a depolarizing shift in steady-state inactivation

Our experiments show that steady-state inactivation of the persistent TTX-R Na^+ current in neonatal neurons is shifted by ~7 mV in a hyperpolarizing direction compared with adult neurons, possibly attributable to the more extensive glycosylation of $Na_v1.9$ channels. To test this hypothesis, we examined the effects of neuraminidase treatment on the voltage dependence of steady-state inactivation of the persistent TTX-R Na^+ current in neonatal DRG neurons. The mean $V_{1/2}$ values and slopes obtained from neonatal DRG neurons after enzymatic desialidation were −47.1 ± 1.0 mV and 5.0 ± 0.6 mV/*e*-fold, respectively. Enzymatic treatment produced a significant ($p < 0.001$) depolarizing shift (8 mV) in the $V_{1/2}$ for steady-state inactivation of the persistent TTX-R Na^+ current (Fig. 6*C*, *filled squares*; Table 1). Desialidation, however, had no significant effects ($p > 0.05$) on the slope for steady-state inactivation of neonatal TTX-R persistent Na^+ current.

Enzymatic desialidation does not shift steady-state activation and inactivation of the persistent TTX-R Na^+ current in adult DRG neurons

Because adult $Na_v1.9$ channels are glycosylated but to a lesser extent than the neonatal channel, we wanted to test whether

←

Table 1. Voltage-dependent activation and steady-state inactivation of $Na_v1.9$ Na^+ current in control and desialidated DRG neurons

	Activation		Inactivation	
Persistent TTX-R Na^+ current	$V_{1/2}$ (mV)	K (mV/*e*-fold)	$V_{1/2}$ (mV)	K (mV/*e*-fold)
Adult DRG neurons ($n = 30$)	-57.3 ± 1.1	6.2 ± 0.5	-48.2 ± 1.33	6.5 ± 0.7
Neuraminidase pretreated adult DRG neurons ($n = 16$)	-57.7 ± 1.8 ($p > 0.05$)	7.7 ± 1.5 ($p > 0.05$)	-50.5 ± 1.0 ($p > 0.05$)	6.40 ± 1.3 ($p > 0.05$)
Neonatal DRG neurons ($n = 29$)	-54.2 ± 1.2	6.62 ± 0.4	-55.2 ± 1.3	6.5 ± 0.4
Neuraminidase pretreated neonatal DRG neurons ($n = 15$)	-57.5 ± 2.2 ($p > 0.05$)	5.8 ± 0.80 ($p > 0.05$)	-47.1 ± 1.0 ($p < 0.001$)	5.0 ± 0.6 ($p > 0.05$)

desialidation affects channel gating. Neuraminidase treatment of adult DRG cultures did not result in a significant change of the $V_{1/2}$ and the slope values for activation and steady-state inactivation ($n = 16$) (Fig. 6B,C, *open squares*) from the values obtained in control neurons (Fig. 6*B*,*C*, *open circles*; Table 1). The persistent TTX-R Na^+ current density and capacitance of the adult DRG neurons after the neuraminidase treatment are 0.62 ± 0.1 nA/pF and 21.14 ± 1.6 pF, respectively, which are similar to those obtained in adult control neurons.

DISCUSSION

We show in this study that Na channel $Na_v1.9$ exists in two glycosylated states during late embryonic and early postnatal stages but only in the less glycosylated state subsequently. Using patch clamp, we show that the current density, current–voltage relationship, and voltage dependence of activation of the persistent TTX-R Na^+ current are similar in neonatal and adult DRG neurons. The voltage dependence of steady-state inactivation, however, is hyperpolarized by ~7 mV in neonatal compared with adult DRG neurons. The difference in steady-state inactivation of the persistent TTX-R Na^+ current is attributable to sialidation of the $Na_v1.9$ channel at neonatal stages. Enzymatic desialidation of neonatal (P0–P3) DRG neurons converts the persistent TTX-R Na^+ current to the adult type.

Adult DRG neurons express six Na channels (Black et al., 1996; Dib-Hajj et al., 1998), including the TTX-R $Na_v1.8$/SNS (Akopian et al., 1996) and $Na_v1.9$/NaN (Dib-Hajj et al., 1998). A number of TTX-S Na channels undergo developmentally regulated and mutually exclusive alternative splicing of exon 5 without a change in the protein size (Sarao et al., 1991; Gustafson et al., 1993; Belcher et al., 1995; Plummer et al., 1997) or of exon 18, which produces a truncated two-domain protein (Plummer et al., 1997). In contrast, Scn11a, the gene encoding $Na_v1.9$, does not contain alternative exons 5N and 18N (Dib-Hajj et al., 1999b). Neonatal and adult $Na_v1.9$ transcripts encoding the variable regions of this channel, which include the N and C termini and interdomain cytoplasmic loops, have similar lengths and sequences. The presence of two $Na_v1.9$ immunoreactive proteins, therefore, indicates post-translational modification of the channel.

We show in this study that $Na_v1.9$ channel undergoes developmentally regulated post-translational processing. Na channels from rat brain and skeletal and cardiac muscle are glycosylated (Barchi et al., 1980; Miller et al., 1983; Messner and Catterall, 1985; Schmidt and Catterall, 1986, 1987; Cohen and Barchi, 1993). Immunoblot analysis shows that $Na_v1.9$ is present in two glycosylated forms around and shortly after birth. The observed molecular weight of $Na_v1.9$ in adult neurons is ~5% higher than the predicted molecular weight of 201 kDa (Dib-Hajj et al., 1998). The extra mass of adult $Na_v1.9$ is attributable to limited glycosylation that is evident by the change in its mobility after PNGase treatment. The exact nature of the sugar group on this protein is not known, and, if sialic acid is present, it does not produce a detectable effect on gating of $Na_v1.9$ in adult neurons.

The ~210 kDa protein is the only detectable form of the channel in adult DRG neurons, and an immunoreactive protein of similar size is also present in neonatal tissue. Limited glycosylation of $Na_v1.9$ in adult tissue may modulate the stability and surface expression of the channel complex. Cotranslational glycosylation has been shown to be important for the proper folding, subsequent channel modification, and interaction with auxiliary subunits of rat brain Na channel α-subunits (Schmidt and Catterall, 1987). The heavier neonatal form of $Na_v1.9$ indicates more extensive processing of the glycocalyx. Sialic acid residues account for the bulk of the sugar content of eel and rat brain and skeletal muscle Na channels (Miller et al., 1983; Messner and Catterall, 1985). Metabolic inhibition of sialic acid addition or enzymatic desialidation does not affect the assembly or surface expression of rat brain Na channels (Schmidt and Catterall, 1987); rather, it modifies their gating properties (Recio-Pinto et al., 1990; Bennett et al., 1997; Zhang et al., 1999). Consistent with the presence of sialic acid residues in the neonatal form of $Na_v1.9$ is the finding that enzymatic desialidation of neonatal DRG cultures changes the properties of the persistent TTX-R Na^+ current.

Heavier glycosylation of neonatal $Na_v1.9$ is consistent with the presence of sialic acid that affects gating properties of this channel. Neonatal persistent TTX-R Na^+ current inactivates at a more hyperpolarized potential compared with that in adult neurons. Treatment of DRG cultures with neuraminidase shifts steady-state inactivation of persistent TTX-R Na^+ current by ~8 mV in a depolarized direction in neonatal but not adult neurons. The effect of neuraminidase treatment indicates that sialic acid contributes to the heavier glycosylation of the neonatal channel and is responsible for the shift in inactivation. The observation that desialidation does not shift the voltage dependence of steady-state inactivation for adult persistent TTX-R Na^+ current is consistent with the limited glycosylation of adult $Na_v1.9$, including a reduced sialic acid component. Alternatively, sialic acid residues may be present in the $Na_v1.9$ Na channels but in a locus that is not proximal to the inactivation gate.

Desialidation did not cause a depolarizing shift in activation of the neonatal persistent TTX-R Na^+ current. In contrast, previ-

ous studies on rat $Na_v1.4$ and human $Na_v1.5$ showed that neuraminidase pretreatment caused a depolarizing shift (~10 mV) of $V_{1/2}$ for activation of these channels (Bennett et al., 1997; Zhang et al., 1999). The reasons for this discrepancy are not clear. These previous studies reported different effects of desialidation on the steady-state inactivation of $Na_v1.4$. Whereas Bennett et al. (1997) reported an ~10 mV depolarizing shift in the steady-state inactivation of $Na_v1.4$, Zhang et al. (1999) reported an ~4 mV hyperpolarizing shift. Desialidation of human $Na_v1.5$ expressed in HEK 293 cell lines and mouse $Na_v1.5$ in native cardiac myocytes produces different effects on the voltage dependence of steady-state inactivation (Zhang et al., 1999; Ufret-Vincenty et al., 2001); desialidation causes an ~10 mV depolarizing shift in human Nav1.5 but an ~8 mV hyperpolarizing shift in mouse $Na_v1.5$. These differences are likely attributable to the cell background rather than a species difference. Cummins et al. (2001) demonstrated that the electrophysiological properties of a Na channel can differ depending on the cell type in which it is expressed. The disagreement between the results of Bennett et al. (1997), Zhang et al. (1999), and Ufret-Vincenty et al. (2001) points to the potential risk of extrapolating results from cell lines to expression in the native environment.

Alternatively, the inability of desialidation to change voltage dependence of activation of $Na_v1.9$ may reflect isoform-specific differences. Although $Na_v1.9$ and $Na_v1.5$ have a similar distribution of N-glycosylation motifs, their gating properties are significantly different (Cummins et al., 1999). Changing external calcium concentration causes nonequivalent shifts on the voltage dependence of channel gating (Frankenhaeuser and Hodgkin, 1957). If sialic acid residues are heterogeneously distributed and if different channel gating domains lie in different parts of the resulting nonuniform transmembrane electric field, differential effects on particular gating behaviors may occur that could depend on the degree or pattern of sialic acid in the glycocalyx. Negative charges in the vicinity of different S4 voltage sensors may have a differential effect on the gating of the channel. Reduced positive charges in the S4 segments of domains II and III of $Na_v1.9$ may underlie the significantly different gating properties of this channel compared with $Na_v1.4$ and $Na_v1.5$ (Cummins et al., 1999; Dib-Hajj et al., 1999a). Also, whereas $Na_v1.4$ currents can be modeled by a Hodgkin–Huxley type equation using three activation particles and one inactivation particle, $Na_v1.9$ currents are best fit with one activation and one inactivation particle (Herzog et al., 2001). It is not unreasonable, therefore, to suggest that desialidation will have a different effect if sialic residues in neonatal $Na_v1.9$ are clustered around the inactivation gate but not the activation gate.

$Na_v1.9$ produces a persistent TTX-R current with wide overlap between activation and steady-state inactivation (Cummins et al., 1999; Dib-Hajj et al., 1999a). Our biophysical studies suggest that, as a result of its voltage dependence and persistent kinetics, $Na_v1.9$ plays an important role in setting the membrane resting potential and in subthreshold electrogenesis (Herzog et al., 2001). The present results demonstrate that the heavily glycosylated neonatal channel inactivates at more hyperpolarized potentials compared with adult channels. Because neonatal $Na_v1.9$ has less of an overlap between its activation and inactivation, neonatal Nav1.9 might be expected to contribute a smaller depolarizing influence on resting potential and a smaller amplification of depolarizing inputs. Different properties of neonatal and adult $Na_v1.9$ channels may thus cause sensory neurons to respond differently to similar stimuli.

REFERENCES

Akopian AN, Sivilotti L, Wood JN (1996) A tetrodotoxin-resistant voltage-gated sodium channel expressed by sensory neurons. Nature 379:257–262.

Barchi RL, Cohen SA, Murphy LE (1980) Purification from rat sarcolemma of the saxitoxin-binding component of the excitable membrane sodium channel. Proc Natl Acad Sci USA 77:1306–1310.

Beckh S, Noda M, Lübbert H, Numa S (1989) Differential regulation of three sodium channel messenger RNAs in the rat central nervous system during development. EMBO J 8:3611–3616.

Belcher SM, Zerillo CA, Levenson R, Ritchie JM, Howe JR (1995) Cloning of a sodium channel alpha subunit from rabbit Schwann cells. Proc Natl Acad Sci USA 92:11034–11038.

Bennett E, Urcan MS, Tinkle SS, Koszowski AG, Levinson SR (1997) Contribution of sialic acid to the voltage dependence of sodium channel gating. A possible electrostatic mechanism. J Gen Physiol 109:327–343.

Black JA, Dib-Hajj S, McNabola K, Jeste S, Rizzo MA, Kocsis JD, Waxman SG (1996) Spinal sensory neurons express multiple sodium channel alpha-subunit mRNAs. Mol Brain Res 43:117–131.

Catterall WA (2000) From ionic currents to molecular mechanisms: the structure and function of voltage-gated sodium channels. Neuron 26:13–25.

Cohen SA, Barchi RL (1993) Voltage-dependent sodium channels. Int Rev Cytol 137C:55–103.

Cummins TR, Dib-Hajj SD, Black JA, Akopian AN, Wood JN, Waxman SG (1999) A novel persistent tetrodotoxin-resistant sodium current in SNS-null and wild-type small primary sensory neurons. J Neurosci 19:RC43(1–5).

Cummins TR, Black JA, Dib-Hajj SD, Waxman SG (2000) Glial-derived neurotrophic factor upregulates expression of functional SNS and NaN sodium channels and their currents in axotomized dorsal root ganglion neurons. J Neurosci 20:8754–8761.

Cummins TR, Aglieco F, Renganathan M, Herzog RI, Dib-Hajj SD, Waxman S (2001) Nav1.3 sodium channels: rapid repriming and slow closed-state inactivation display quantitative differences following expression in a mammalian cell line and in spinal sensory neurons. J Neurosci 21:5952–5961.

Dib-Hajj S, Black JA, Felts P, Waxman SG (1996) Down-regulation of transcripts for Na channel alpha-SNS in spinal sensory neurons following axotomy. Proc Natl Acad Sci USA 93:14950–14954.

Dib-Hajj SD, Tyrrell L, Black JA, Waxman SG (1998) NaN, a novel voltage-gated Na channel, is expressed preferentially in peripheral sensory neurons and down-regulated after axotomy. Proc Natl Acad Sci USA 95:8963–8968.

Dib-Hajj SD, Tyrrell L, Cummins TR, Black JA, Wood PM, Waxman SG (1999a) Two tetrodotoxin-resistant sodium channels in human dorsal root ganglion neurons. FEBS Lett 462:117–120.

Dib-Hajj SD, Tyrrell L, Escayg A, Wood PM, Meisler MH, Waxman SG (1999b) Coding sequence, genomic organization, and conserved chromosomal localization of the mouse gene Scn11a encoding the sodium channel NaN. Genomics 59:309–318.

Felts PA, Yokoyama S, Dib-Hajj S, Black JA, Waxman SG (1997) Sodium channel alpha-subunit mRNAs I, II, III, NaG, Na6 and HNE (PN1)—different expression patterns in developing rat nervous system. Mol Brain Res 45:71–82.

Fitzgerald M, Wall PD, Goedert M, Emson PC (1985) Nerve growth factor counteracts the neurophysiological and neurochemical effects of chronic sciatic nerve section. Brain Res 332:131–141.

Fjell J, Hjelmstrom P, Hormuzdiar W, Milenkovic M, Aglieco F, Tyrrell L, Dib-Hajj S, Waxman SG, Black JA (2000) Localization of the tetrodotoxin-resistant sodium channel NaN in nociceptors. NeuroReport 11:199–202.

Frankenhaeuser B, Hodgkin AL (1957) The action of calcium on the electrical properties of squid axon. J Physiol (Lond) 137:218–244.

Goldin AL (2001) Resurgence of sodium channel research. Annu Rev Physiol 63:871–894.

Goldin AL, Barchi RL, Caldwell JH, Hofmann F, Howe JR, Hunter JC, Kallen RG, Mandel G, Meisler MH, Netter YB, Noda M, Tamkun MM, Waxman SG, Wood JN, Catterall WA (2000) Nomenclature of voltage-gated sodium channels. Neuron 28:365–368.

Gustafson TA, Clevinger EC, O'Neill TJ, Yarowsky PJ, Kreuger BK (1993) Mutually exclusive exon splicing of type III brain sodium channel alpha subunit RNA generates developmentally regulated isoforms in rat brain. J Biol Chem 268:18648–18653.

Herzog RI, Cummins TR, Waxman SG (2001) Role of resistant tetrodotoxin-resistant (TTX-R) sodium currents in modulating dorsal root ganglia (DRG) excitability: a computer simulation and patch-clamp study. J Neurophysiol 86:1351–1364.

Kim HC, Chung MK (1999) Voltage-dependent sodium and calcium currents in acutely isolated adult rat trigeminal root ganglion neurons. J Neurophysiol 81:1123–1134.

Messner DJ, Catterall WA (1985) The sodium channel from rat brain. Separation and characterization of subunits. J Biol Chem 260:10597–10604.

Miller JA, Agnew WS, Levinson SR (1983) Principal glycopeptide of the tetrodotoxin/saxitoxin binding protein from *Electrophorus electricus*: isolation and partial chemical and physical characterization. Biochemistry 22:462–470.

Plummer NW, McBurney MW, Meisler MH (1997) Alternative splicing of the sodium channel SCN8A predicts a truncated two-domain protein in fetal brain and non-neuronal cells. J Biol Chem 272:24008–24015.

Recio-Pinto E, Thronhill WB, Duch DS, Levinson SR, Urban BW (1990) Neuraminidase treatment modifies the function of electroplax sodium channels in planar lipid bilayers. Neuron 5:675–684.

Renganathan M, Cummins TR, Hormuzdiar WN, Black JA, Waxman SG (2000a) Nitric oxide is an autocrine regulator of Na(+) currents in axotomized C-type DRG neurons. J Neurophysiol 83:2431–2442.

Renganathan M, Cummins TR, Hormuzdiar WN, Waxman SG (2000b) alpha-SNS produces the slow TTX-resistant sodium current in large cutaneous afferent DRG neurons. J Neurophysiol 84:710–718.

Roberts RH, Barchi RL (1987) The voltage-sensitive sodium channel from rabbit skeletal muscle. Chemical characterization of subunits. J Biol Chem 262:2298–2303.

Sarao R, Gupta SK, Auld VJ, Dunn RJ (1991) Developmentally regulated alternative RNA splicing of rat brain sodium channel mRNAs. Nucleic Acids Res 19:5673–5679.

Schaller KL, Caldwell JH (2000) Developmental and regional expression of sodium channel isoform NaCh6 in the rat central nervous system. J Comp Neurol 420:84–97.

Schmidt JW, Catterall WA (1986) Biosynthesis and processing of the alpha subunit of the voltage-sensitive sodium channel in rat brain neurons. Cell 46:437–444.

Schmidt JW, Catterall WA (1987) Palmitylation, sulfation, and glycosylation of the alpha subunit of the sodium channel. Role of post-translational modifications in channel assembly. J Biol Chem 262:13713–13723.

Shi G, Trimmer JS (1999) Differential asparagine-linked glycosylation of voltage-gated K^+ channels in mammalian brain and in transfected cells. J Membr Biol 168:265–273.

Sleeper AA, Cummins TR, Dib-Hajj SD, Hormuzdiar W, Tyrrell L, Waxman SG, Black JA (2000) Changes in expression of two tetrodotoxin-resistant sodium channels and their currents in dorsal root ganglion neurons after sciatic nerve injury but not rhizotomy. J Neurosci 20:7279–7289.

Ufret-Vincenty CA, Baro DJ, Lederer WJ, Rockman HA, Quinones LE, Santana LF (2001) Role of sodium channel deglycosylation in the genesis of cardiac arrhythmias in heart failure. J Biol Chem 276:28197–28203.

Zhang Y, Hartmann HA, Satin J (1999) Glycosylation influences voltage-dependent gating of cardiac and skeletal muscle sodium channels. J Membr Biol 171:195–207.